

1 **Comparison of source apportionment approaches and analysis of**
2 **non-linearity in a real case model application**

3 Claudio A. Belis¹, Guido Pirovano², Maria Gabriella Villani³, Giuseppe Calori⁴, Nicola Pepe⁴,
4 Jean Philippe Putaud¹

5

6 ¹ European Commission, Joint Research Centre, via Fermi 2748, 21027 Ispra (VA), Italy

7 ² RSE Spa, via Rubattino 54, 20134, Milan, Italy

8 ³ ENEA Laboratory of Atmospheric Pollution, via Fermi 2748, 21027 Ispra (VA), Italy

9 ⁴ ARIANET s.r.l. via Gilino, 9 - 20128 Milan (MI) – Italy

10 *Correspondence to:* Claudio A. Belis (claudio.belis@ec.europa.eu)

11 **Abstract.** The response of particulate matter (PM) concentrations to emission reductions was analysed by assessing
12 the results obtained with two different source apportionment approaches. The brute force (BF) method source impacts,
13 computed at various emission reduction levels using two chemical transport models (CAMx and FARM), were
14 compared with the contributions obtained with the tagged species (TS) approach (CAMx with PSAT module). The
15 study focused on the main sources of secondary inorganic aerosol precursors in the Po Valley (Northern Italy):
16 agriculture, road transport, industry and residential combustion. The interaction terms between different sources
17 obtained from a factor decomposition analysis were used as indicators of non-linear PM₁₀ concentration responses to
18 individual source emission reductions. Moreover, such interaction terms were analysed in the light of the free ammonia
19 / total nitrate gas ratio to determine the relationships between the chemical regime and the non-linearity at selected
20 sites. The impacts of the different sources were not proportional to the emission reductions and such non-linearity was
21 most relevant for 100% emission reduction levels compared with smaller reduction levels (50% and 20%). Such
22 differences between emission reduction levels were connected to the extent to which they modify the chemical regime
23 in the base case. Non-linearity was mainly associated with agriculture and the interaction of this source with road
24 transport and, to a lesser extent, with industry. Actually, the mass concentration of PM₁₀ allocated to agriculture by
25 TS and BF approaches were significantly different when a 100% emission reduction was applied. However, in many
26 situations the non-linearity in PM₁₀ annual average source allocation was negligible and the TS and the BF approaches
27 provided comparable results. PM mass concentrations attributed to the same sources by TS and BF were highly
28 comparable in terms of spatial patterns and quantification of the source allocation for industry, transport and residential
29 combustion. The conclusions obtained in this study for PM₁₀ are also applicable to PM_{2.5}.

30

31

32 1. Introduction

33 Air pollution is the main environmental cause of premature death. Ambient air pollution caused 4.2 million deaths
34 worldwide in 2016, contributing together with indoor pollution to 7.6% of all deaths (WHO, 2018). Air pollution
35 adverse health effects mainly occur as respiratory and cardiovascular diseases (WHO, 2016; EEA 2019). A key
36 element for the design of effective air quality control strategies is the knowledge of the role of different emission
37 sources in determining the ambient concentrations. This is usually referred to as source apportionment (SA) and
38 involves the quantification of the influence of different human activities (e.g. transport, domestic heating, industry,
39 agriculture) and geographical areas (e.g. local, urban, metropolitan areas, countries) to air pollution at a given location.

40 SA modelling studies involving secondary inorganic pollutants are generally based on chemistry transport models
41 (Mircea et al., 2020). Two different SA approaches are commonly used to allocate the mass of pollutants to the
42 different sources by means of chemical transport models:

43 • tagged species (TS) quantifies the **contribution** of emission sources to the concentration of one pollutant at
44 one given location by implementing algorithms to trace reactive tracers. SA studies based on tagging methods have
45 been carried out at both European scale (e.g. Karamchandani et al. 2017; Manders et al., 2017) and urban scale (e.g.
46 Pepe et al. 2019, Pültz, et al., 2019).

47 • brute force (BF or emission reduction impact) is a sensitivity analysis technique which estimates the change
48 in pollutant concentration (impact) that results from a change of one or more emission sources. Sensitivity analysis
49 techniques have been used to estimate the **impact** of different sources on pollution levels (e.g. Kiesewetter et al., 2015;
50 Thunis et al., 2016; Van Dingenen et al., 2018).

51 Even though these approaches are often considered as two alternative SA methods, they actually pursue different
52 objectives: TS aims to account for the mass transferred from the sources to the receptor in a specific area and time
53 window while BF is a sensitivity analysis technique used to estimate the response of the system to changes in
54 emissions. For a detailed discussion, refer to Belis et al. (2020); Mircea et al. (2020); Thunis et al. (2019).

55 Clappier et al. (2017) applied the concept of factor decomposition developed by Stein and Alpert (1993) to investigate
56 the differences between TS and BF using a theoretical example involving three sources. According to these authors,
57 the change in concentration of a given pollutant due to the change in the emissions of three sources A, B and C (ΔC_{ABC})
58 can be described as follows:

$$59 \Delta C_{ABC} = \Delta C_A + \Delta C_B + \Delta C_C + \hat{c}_{AB} + \hat{c}_{AC} + \hat{c}_{BC} + \hat{c}_{ABC} \quad (1)$$

60 Where ΔC_A , ΔC_B and ΔC_C are the variations of concentration of the studied pollutant due to the reduction of the single
61 sources A, B and C, respectively, and those coming from the interactions between these sources denoted by the terms
62 \hat{c}_{AB} , \hat{c}_{AC} , \hat{c}_{BC} and \hat{c}_{ABC} (see Appendix A for details). The interaction terms (\hat{c}) have the same units as the source impacts.

63 In the TS approach, the sum of the contributions of the various sources always matches the total pollutant concentration
64 by design. ($M_{poll} = M_A + M_B + M_C$), while this may be not the case for the BF approach ($\Delta C_{ABC} \neq \Delta C_A + \Delta C_B +$
65 ΔC_C) under certain circumstances (Belis et al., 2020). The interaction terms in eq. 1 measure the consistency between
66 the sum of single emission sources with respect to the contemporary reduction of more than one source in BF, for
67 three sources $\Delta C_{ABC} - (\Delta C_A + \Delta C_B + \Delta C_C)$, which is an indicator of the non-linearity in the response of the pollutant
68 concentration to single source reductions (impacts).

69 There are different situations that may contribute to generating non-linear response when secondary pollutants'
70 precursors are emitted by different sources. They are double counting, chemical regime limited by one precursor,
71 competition between precursors, thermodynamic equilibrium between the secondary pollutant and its precursors, and
72 compensation. A detailed explanation of each of them is provided in Appendix A.

73 In the analysis of a theoretical example with three sources (agriculture, industry and residential), Clappier et al., 2017
74 observed that strong non-linearity is associated with secondary inorganic aerosol (SIA, ammonium nitrate and
75 ammonium sulfate) formation. However, this secondary aerosol may behave linearly or non-linearly depending on the

76 circumstances; for instance, the intensity of the emission reduction, which imposes the need to quantify it for different
77 emission reduction levels (ERLs) (see Section 3.2). Thunis et al. (2015) showed that for yearly average relationships
78 between emission and concentration changes, linearity is often a realistic assumption and consequently, TS and BF
79 methods are expected to provide comparable results, as reported by Belis et al. (2020). The abovementioned
80 considerations suggest the need to monitor whether non-linearity is significant for a given study area and time window.

81 The objective of this study is to identify and quantify the factors leading to non-linear response of PM concentrations
82 to source emission reductions in a real-world situation with significant PM concentrations. To that end, the influence
83 on PM₁₀ concentration of various sources with different chemical profiles were calculated using both the BF approach
84 with two different chemical transport models (CAMx and FARM) and the TS approach using one of these chemical-
85 transport models (CAMx).

86 The results of the simulations were then used to:

- 87 • compare TS contributions with BF impacts
- 88 • analyse the geographical patterns
- 89 • compute interaction terms (of the Stein and Alpert algebraic expression) for the studied sources
- 90 • compare the behaviour of various areas (urban, rural, etc.) with different chemical regimes

91 In this study, the focus is on the non-linearity associated with SIA formation, with particular reference to ammonium
92 nitrate (NH₄NO₃) and ammonium sulfate ((NH₄)₂SO₄). The possible non-linear behaviour of any other PM component
93 (e.g. organics) is beyond the scope of this exercise.

94 2. Materials and methods

95 The Po Valley was selected for this study because of its high levels of particulate matter due to the high emissions of
96 primary pollutants and precursors of SIA, whose high concentrations are also favoured by the stagnation of air masses
97 during the coldest months of the year (Belis et al., 2011, Larsen et al., 2012).

98 The air quality simulations were performed with CAMx (ENVIRON, 2016) and FARM (ARIANET, 2019) chemical
99 transport models (CTMs). Both are open-source modelling systems for multi-scale integrated assessment of gaseous
100 and particulate air pollution. Thanks to their variable spatial resolution they are used for urban to regional scale
101 applications, and simulating the atmospheric chemical reactions of the emitted precursors they allow reconstructing
102 the formation of most of the secondary compounds, including the constituents of particulate matter. CAMx is widely
103 used to assess the influence of pollution sources on air quality in a particular domain. The PM Source Apportionment
104 Technology (PSAT) ; Yarwood et al., 2004) implemented in CAMx offers the choice between several SA approaches,
105 which allows users to easily compare e.g. TS vs BF methods for the estimation of source contributions to pollutant
106 concentrations using the same model. In addition, the application of the BF method with FARM made it possible to
107 evidence the structural behaviours that are less dependent on the specific model formulation and consequently to
108 obtain results of more general value.

109 The application of such CTMs required the implementation of a comprehensive modelling system (e.g. Pepe et al.,
110 2019), including specific tools aiming at creating the three main input categories: meteorological fields, emissions and
111 boundary conditions.

112 Both modelling systems were applied for the reference year 2010 over Northern Italy (Figures S1 and S2) considering
113 a computational domain that covers a 580 x 400 km² region, with a 5 km grid step. For the meteorological model WRF
114 (Skamarock et al., 2008) three nested grids were used, the largest one covering Europe and Northern Africa, and the
115 innermost one corresponding to Italy and Po Valley, respectively. The three meteorological domains have 45, 15, and
116 5 km grid resolution. For CTMs only the innermost WRF nested grid was used. Both CTMs were setup using the same
117 input meteorological data and horizontal grid structure of WRF. CTMs vertical grid was defined collapsing the 27

118 vertical layers used by WRF into 14 layers, while keeping identical the layers up to 1 km above ground level; in
119 particular, the first layer thickness was up to about 25 m from the ground like the corresponding WRF layer.

120 In CAMx, homogenous gas phase reactions of nitrogen compounds and organic species were reproduced through the
121 CB05 mechanism (Yarwood et al., 2005). The aerosol scheme was based on two static modes (coarse and fine).
122 Secondary inorganic compounds evolution were described by the thermodynamic model ISORROPIA (Nenes et al.,
123 1998), while SOAP (ENVIRON, 2011) was used to describe secondary organic aerosol formation. Meteorological
124 input data were provided by WRF and were completed by OMI satellite data (<http://toms.gsfc.nasa.gov>), including
125 ozone vertical content and aerosol turbidity. Vertical turbulence coefficients (Kv) were computed using O'Brien
126 scheme (O'Brien, 1970), but adopting two different minimum Kv values for rural and urban areas, so to consider heat
127 island phenomena and increased roughness of built areas.

128 FARM simulations were performed using the SAPRC-99 gas-phase chemical mechanism (Carter, 2000) and a three-
129 mode aerosol scheme (Binkowski and Roselle, 2003) including microphysics, ISORROPIA for thermodynamic
130 equilibrium of inorganic species and SORGAM (Schell et al., 2001) for secondary organic aerosol formation.
131 Meteorological input from WRF was complemented by Kv computed using Lange (1989) parameterisation.

132 Emissions were derived from inventory data at three different levels: European Monitoring and Evaluation Programme
133 data (EMEP, <http://www.ceip.at/emission-data-webdab/emissions-used-in-emepmodels/>) available over a regular grid
134 of 50 x 50 km² and ISPRA Italian national inventory data ([http://www.sinanet.isprambiente.it/it/sia-](http://www.sinanet.isprambiente.it/it/sia-ispra/inventaria/disaggregazione-dellinventario-nazionale-2010)
135 [ispra/inventaria/disaggregazione-dellinventario-nazionale-2010](http://www.sinanet.isprambiente.it/it/sia-ispra/inventaria/disaggregazione-dellinventario-nazionale-2010)) which provides a disaggregation by province.
136 Moreover, regional inventories data based on INEMAR methodology (INEMAR – ARPA Lombardia, 2015) provided
137 detailed emissions data at municipality level for the four administrative regions of Lombardy, Piedmont, Veneto and
138 Emilia Romagna.

139 Each emission inventory was processed to obtain the hourly time pattern of the emissions. For the CAMx simulations
140 this was accomplished using the Sparse Matrix Operator for Kernel Emissions model (SMOKE v3.5) (UNC, 2013).
141 Temporal disaggregation was based on monthly, daily and hourly profiles deducted by CHIMERE (INERIS, 2006)
142 and EMEP models from Institute of Energy Economics and the Rational Use of Energy (IER) project named
143 GENEMIS (Pernigotti et al., 2013). Similar emission inventories processing was performed for FARM using Emission
144 Manager pre-processing system (ARIA Technologies and ARIANET, 2013).

145 Initial and boundary conditions were taken from a parent CAMx simulation covering the whole Italy and driven by
146 MACC-II system (<http://www.gmes-atmosphere.eu/services/qaqc/>) that provides 3D global concentrations fields.

147 **Table 1: Macro-sectors according to EEA SNAP classification for emission inventories used to define air pollution sources**
148 **in this study**

Source: SNAP Macrosector	SNAP Macrosector number	ABBREVIATION used in this study
Energy industry	1	OTHER
Residential and commercial/institutional combustion	2	RES
Industry (combustion & processes)	3 and 4	IND
Fugitive emissions from fuels	5	OTHER
Product use including solvents	6	OTHER
Road transport	7	TRA
Non-road transport	8	OTHER
Waste treatment	9	OTHER
Agriculture	10	AGR

149
150 The CAMx modelling system was applied with the previously described setup in order to perform a TS run (with
151 PSAT) and three sets of BF runs with 100%, 50% and 20% emission reduction levels (ERLs) while FARM was used
152 to produce two sets of BF runs with 50% and 20% ERLs. Due to the high number of runs needed to apply the Stein
153 and Alpert decomposition only few sources were selected (Table 1). Originally, the study focused on the same system

154 of three sources (AGR, IND, RES) as the study by Clappier et al. (2017). However, due to the small non-linearity
 155 associated with RES the focus was then shifted to a ternary system including AGR, TRA and IND. In total, 41 runs
 156 were performed keeping all inputs as the base case (BC), except for emissions that were modified according to the
 157 scheme reported in Table 2.

158 In this study, the interactions between sources AGR, TRA and IND are mainly analysed. Additional runs were
 159 executed using FARM at 50% and 20% ERLs to test also the impacts and interactions of RES with the previous ones.

160 **Table 2: Sets of simulations performed in this study to compute the factor decomposition (Stein and Alpert, 1993). Every**
 161 **set is named after the used CTM and ERL.**

Simulation set	CAMx 100%	CAMx 50%	CAMx 20%	FARM 50%	FARM20%
Reduced sources					
No reduction	Base case CAMx			Base case FARM	
AGR	x	x	x	x	x
IND	x	x	x	x	x
TRA	x	x	x	x	x
RES				x	x
AGR-IND	x	x	x	x	x
AGR-TRA	x	x	x		x
IND-TRA	x	x	x	x	x
RES-IND				x	x
RES-TRA				x	
RES-AGR				x	
AGR-IND-TRA	x	x	x		x
RES-IND-TRA				x	x

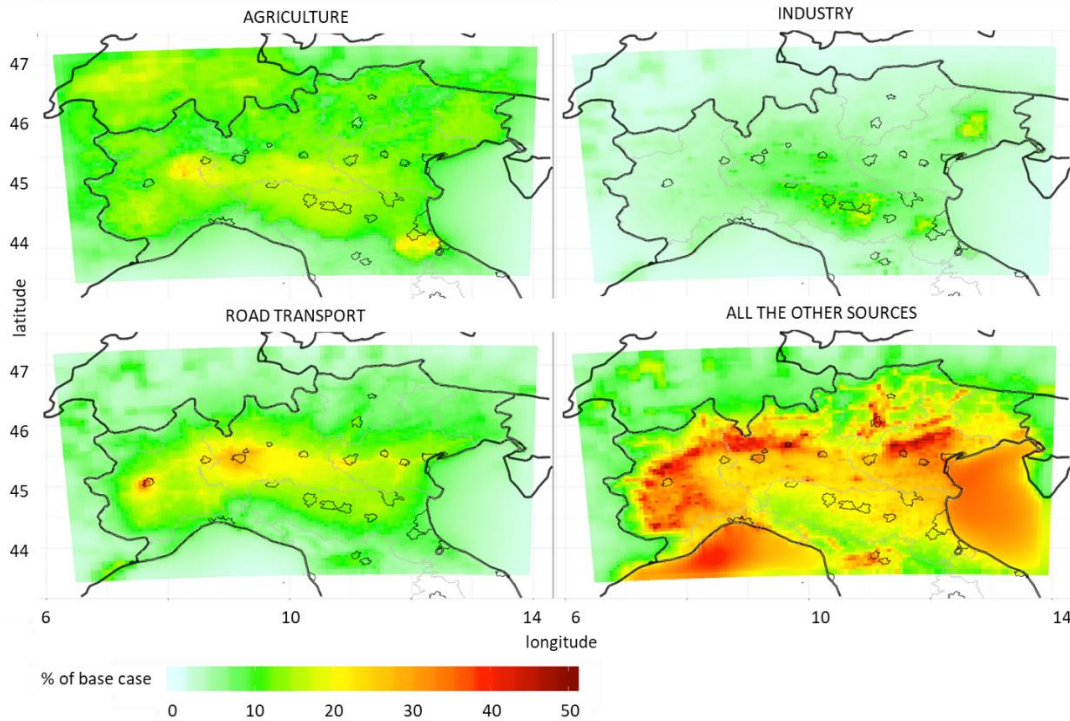
162 3. Results and Discussion

163 3.1 Comparison between source apportionment TS and BF approaches

164 The yearly average PM₁₀ concentrations in the CAMx and FARM base case runs are shown in Figures S1 and S2 of
 165 the supplementary material. Figure 1 shows the relative contributions of the modelled PM₁₀ sources using the TS
 166 approach (CAMx-PSAT). The contributions of AGR are distributed across the entire Po Valley with maximum levels
 167 in the centre and hot spots to the NW and SE. The IND contributions are the highest to the south, SE and NE of the
 168 study area. The TRA contributions to PM₁₀ are the highest in the main urban areas, in particular Milan and Turin, and
 169 along the main highways (e.g. A4 Turin - Venice). The highest contributions of all the other remaining sources
 170 (OTHER) are observed in the Pre-alpine area and in the Alpine valleys (including some areas in the Apennines) where
 171 the average PM₁₀ levels are lower than the Po Valley (Figures S1 and S2) and RES is an important source (see below).

172 The annual average impacts of AGR, TRA and IND on PM₁₀ derived by BF approach with CAMx and FARM for
 173 different emission reduction levels (ERLs) are shown in Figure 2 while those of RES are shown in Figure S3. In a
 174 linear situation the impacts allocated to each source decrease proportionally to the intensity of the emission reduction
 175 ($\Delta C_{100\%} = 2 \Delta C_{50\%} = 5 \Delta C_{20\%}$). For that reason, the impacts at the 100% ERL can be compared directly with TS
 176 contributions while those of 50% and 20% must be multiplied by factor 2 and 5, respectively. The linearity between
 177 different ERLs is discussed in Section 3.2. To facilitate the comparison between different models, impacts are
 178 expressed as percentage of the base case in these figures. In Figure 2, the highest impacts are those of AGR followed
 179 by TRA and IND. The output resulting from CAMx and FARM for the 50% and 20% ERLs present similar levels and
 180 geographical patterns. Most of the highest impacts of AGR at 100% ERL are observed in or near the areas of high
 181 NH₃ emissions (Figure S4), in which also TS points out high contributions of this source (Figure 1). However, in these
 182 areas the BF impacts are nearly twice the TS contributions reported in Figure 1 (see also Figure 3, top left). Such high
 183 levels could be attributed to a near double counting effect which is dominant only at this ERL because the effect of
 184 limited chemical regime cannot be observed at 100% reduction (see Appendix A Section A2.2). At 50% and 20%

185 ERLs the impacts are lower than the 100% ERL, because of the limited regime, and the highest ones are located in
 186 the mountainous areas (Alps and Apennines). Such pattern is likely due to the low emissions of the SIA precursors
 187 (NH_3 , NO_x and SO_2) (Figure S4) and the modest base case PM_{10} concentrations in these areas. For IND and TRA, the
 188 geographical patterns of BF are comparable to those of TS (Figure 1, Figure 3 left) and do not vary significantly
 189 between the different ERLs, as discussed in Section 3.2. The only remark is that FARM presents higher TRA impacts
 190 in the subalpine areas compared to CAMx, irrespective of the used SA approach.



191
 192 **Figure 1: Annual contributions of the PM_{10} sources over the Po Valley area according to tagged species (TS) approach as**
 193 **computed by CAMx PSAT. The grey lines indicate the boundaries of the regions and the polygons represent the municipal**
 194 **areas of the main cities.**

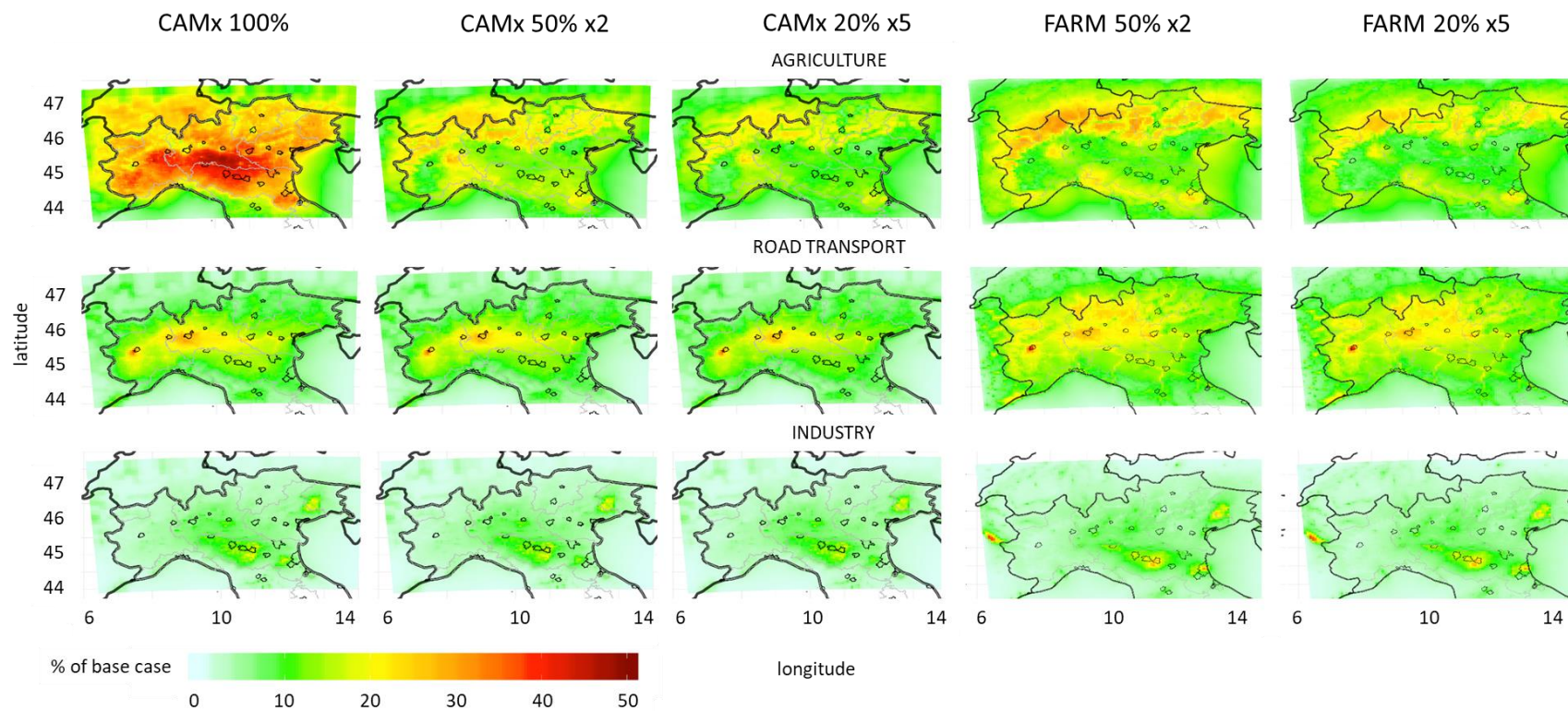
195 As shown in Figure 3, the single grid cell annual average of BF impacts on PM_{10} by IND and TRA plotted versus the
 196 TS contributions are arranged on a line close to the identity indicating that BF and TS approaches lead to similar
 197 results for these two sources. A similar behaviour is observed in all the ERLs even though the BF impacts estimated
 198 with FARM present a higher dispersion than those obtained with CAMx. Such closer relationship between TS (CAMx-
 199 PSAT) and CAMx BF results is likely a consequence of both being results of the same model. On the contrary, the
 200 impacts of AGR on PM_{10} at 100% ERL are more than twice the TS contributions in most grid cells, which is due to
 201 the much greater AGR BF impacts on sulfate and nitrate than TS contributions at this ERL (Figures S5 and S6,
 202 respectively). Such non-linear behaviour is associated with a situation near to double counting, which results in
 203 negative interaction terms, and for nitrate, also to the NH_4NO_3 equilibrium, since both effects lead to BF impacts
 204 higher than TS contributions (Appendix A).

205 Despite the comparable range of BF impacts and TS contributions of AGR on PM_{10} at 50% and 20% ERLs (Figure
 206 3), there is a considerable dispersion around the regression line (R^2 between 0.65 and 0.72) indicating spatial
 207 heterogeneity. In addition, impacts at 20% ERL present a slightly lower slope with respect to TS contributions than
 208 those at 50% ERL. Also AGR BF impacts on nitrate present non-linear high values at 50% and 20% ERLs, which are
 209 however compensated by ammonium impacts which are much lower than TS contributions (Figures S6 and S7,
 210 respectively). The greater difference observed between TS and BF at 100% ERL for AGR compared to TRA and IND
 211 are in part due to AGR being the only significant source of NH_3 in the domain. Consequently, a 100% reduction of
 212 AGR implies an almost complete abatement of NH_3 , while 100% reduction of TRA or IND does not reduce NO_x and

213 SO₂ emissions completely (compensation effect). The reported differences between AGR TS contributions and BF
214 impacts on PM₁₀ concentrations are due to the way in which the two approaches allocate ammonium, nitrate and
215 sulfate to this source. TS allocates secondary constituents according to the mass of precursors deriving from each
216 source (Mircea et al., 2020; Yarwood et al., 2004). Therefore, for TS the contribution of AGR is close to the mass
217 fraction of ammonium in PM₁₀ and very little nitrate and sulfate is allocated to this source, since SO₂ and NO_x
218 emissions from AGR are small compared to those from IND and TRA. On the contrary, BF allocates these constituents
219 on the basis of the amount of NH₄NO₃ and/or (NH₄)₂SO₄ which is not formed when such sources are reduced.
220 Consequently, considerable nitrate and sulfate are allocated to AGR by BF, even though are not physically emitted by
221 this source, because there is no formation of NH₄NO₃ and/or (NH₄)₂SO₄ in the absence of NH₃ emissions from AGR.

222 Even in the cases where BF impacts and TS contributions to PM₁₀ are linear and close to identity, PM₁₀ constituents
223 may not behave in the same way. Sometimes, the linearity observed in PM₁₀ is the result of a compensation between
224 constituents for which BF impacts > TS contributions and others for which BF impacts < TS contributions. A good
225 example is TRA, whose annual BF impacts on PM₁₀ are aligned with TS contributions (Figure 3). However, the
226 ammonium impacts from this source are highly non-linear and larger than TS contributions (Figures S7), sulfate
227 impacts are quite non-linear and can be either larger or smaller compared to TS contributions (Figure S5), while nitrate
228 impacts are rather linear and slightly lower than TS contributions (Figure S6). A similar situation is observed for
229 nitrate and ammonium impacts from IND, with the difference that in this case sulfate, a component for which this
230 source is dominant, is rather linear.

231 The non-linearity between TS and BF source apportionment of PM₁₀ secondary inorganic constituents observed in
232 Figures S5 - S7 occur when the BF and TS approaches do not allocate these compounds to the same sources. For
233 instance, high non-linearity is observed for BF impacts of TRA and IND on ammonium because it is emitted almost
234 exclusively by AGR, while BF methods allocate impacts on ammonium to TRA and IND due to the atmospheric
235 reactions between NH₃ and HNO₃ or H₂SO₄, which are mainly emitted from TRA and IND, respectively. A similar
236 situation is observed for AGR impacts on sulfate and nitrate. TS allocates a negligible share of these compounds to
237 AGR (proportional to SO₂ and NO_x emissions from AGR only), while the BF method allocates them to this source
238 proportionally to the (NH₄)₂SO₄ and NH₄NO₃ concentration variations, respectively.

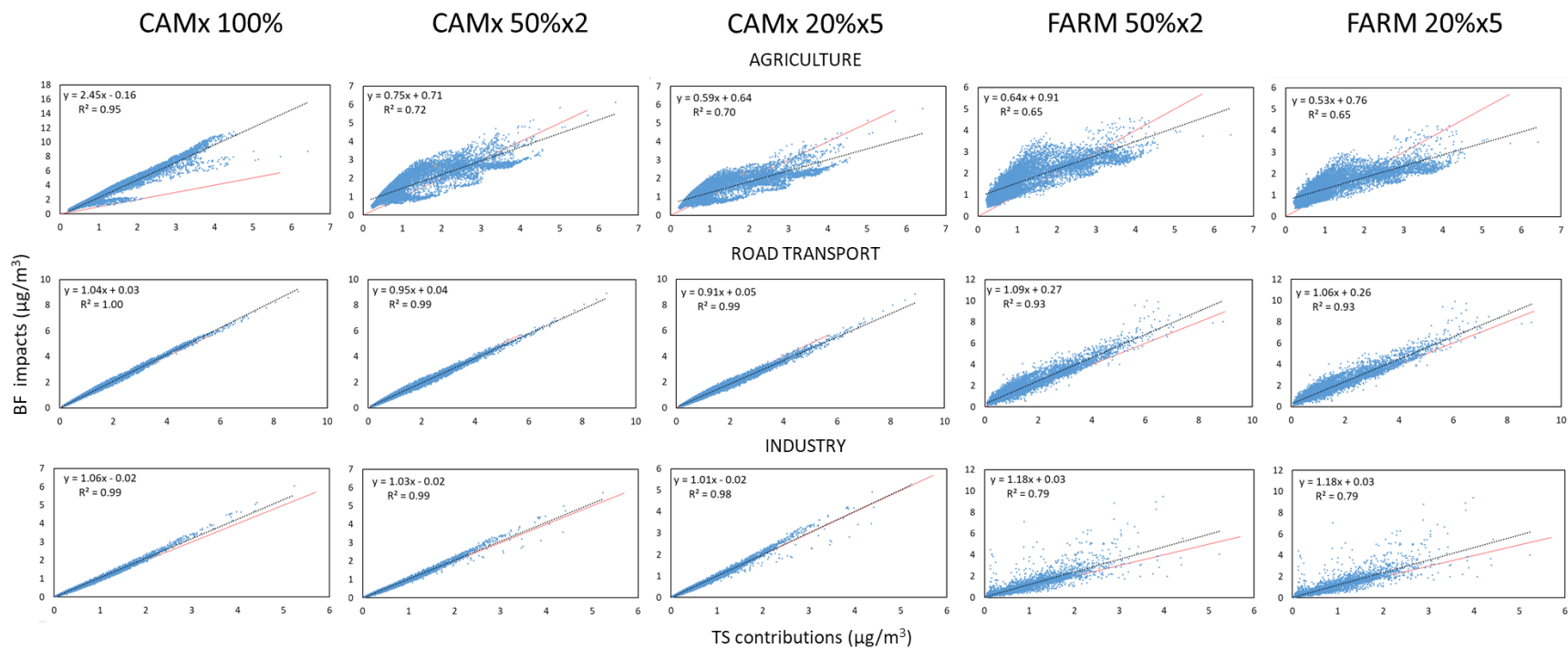


240

241 **Figure 2: Annual average impacts of AGR, TRA and IND expressed as percentage of the base case. From left to right CAMx 100%, 50% and 20% emission reduction**
 242 **levels and FARM 50% and 20% emission reduction levels. For a direct comparison of the linearity between the different ERLs, the impacts of 50% and 20% are multiplied**
 243 **by 2 and 5, respectively.**

244

245



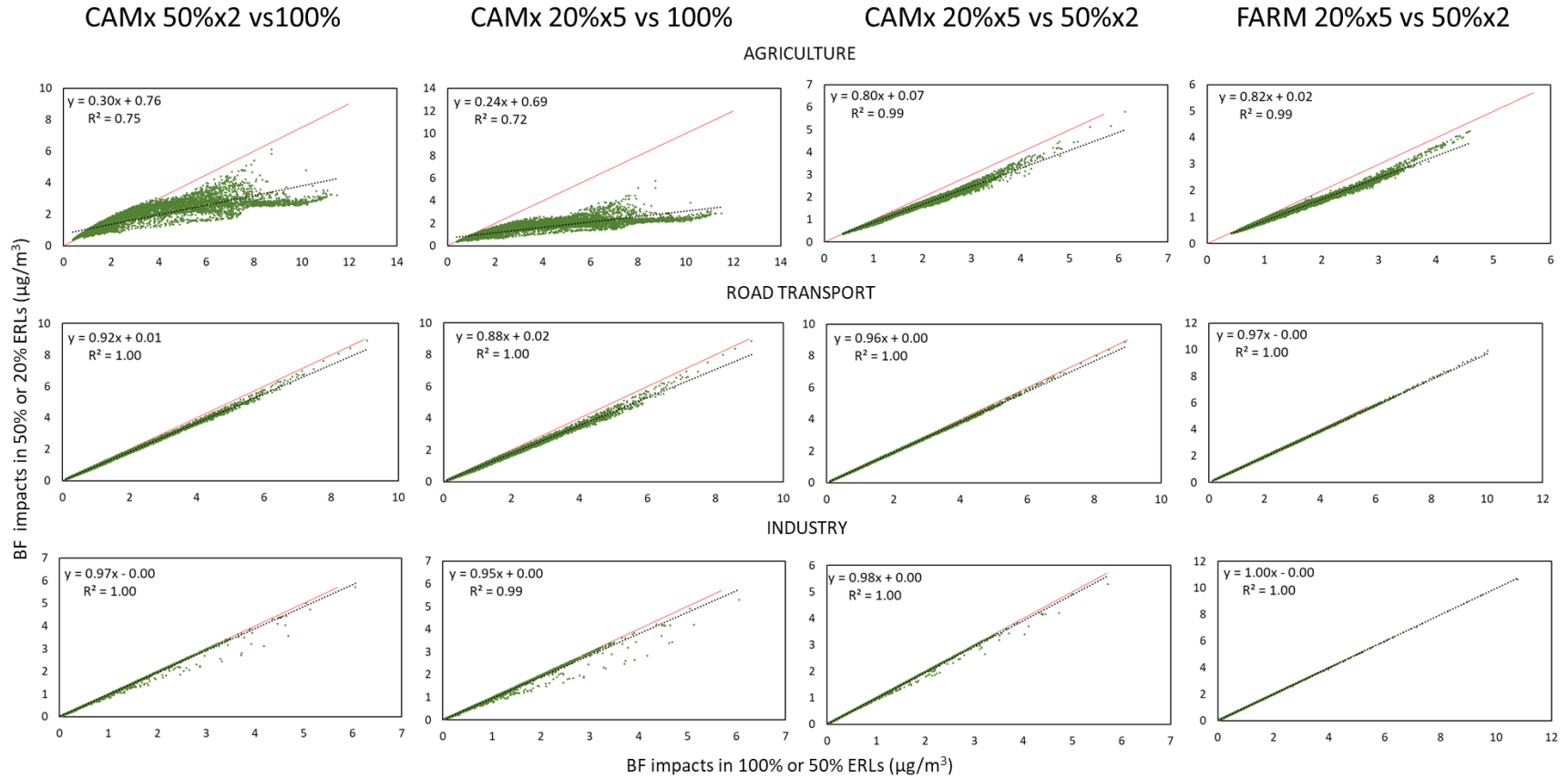
247

248 **Figure 3: Scatter plots of the single grid cell annual average BF source impacts (CAMx and FARM) on PM₁₀ versus the TS contributions (CAMx -PSAT) for 100%, 50%**
 249 **(multiplied by 2) and 20% (multiplied by 5) ERLs for AGR, TRA and IND. Dotted line: regression; red line: identity.**

250

251

252



253

254 **Figure 4: Scatter plots of the single grid cell BF source impacts (CAMx and FARM) on PM₁₀ between the 100%, 50% (multiplied by 2) and 20% (multiplied by 5) ERLs**
 255 **for AGR, TRA and IND. Dotted line: regression; red line: identity**

256 The analysis of the impacts reported in this section clearly points out AGR as the source mostly associated with the
257 non-linear response of BF impacts with respect to TS.

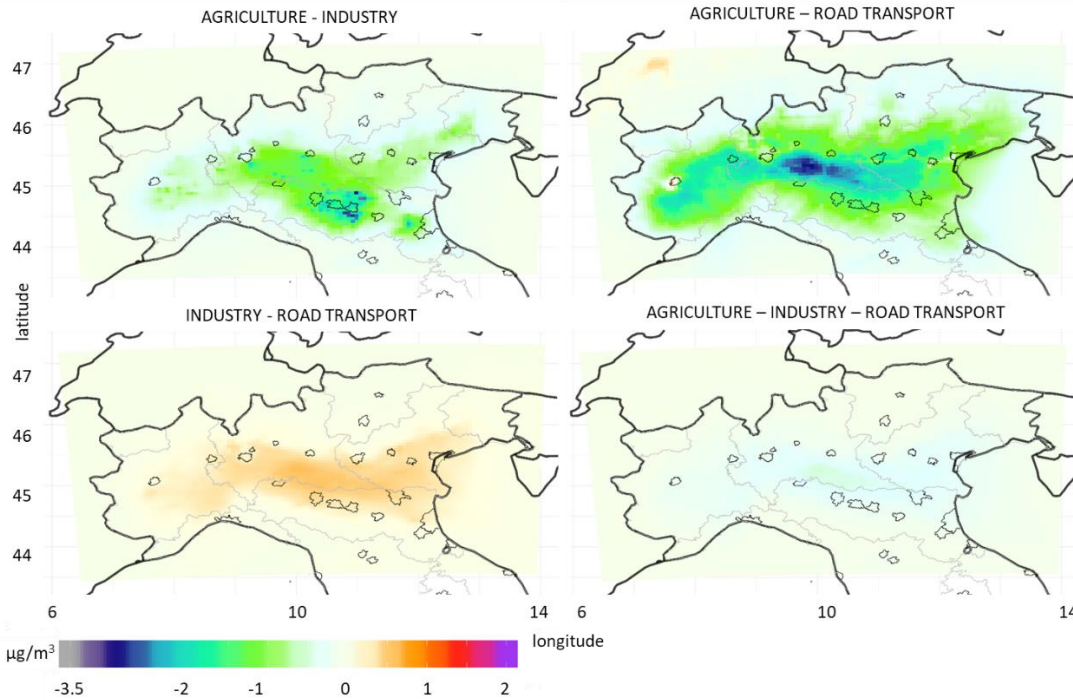
258 3.2 Non linearity between different ERLs

259 In this section the connection between the magnitude of the emission reduction and the BF source impacts on PM₁₀ is
260 analysed more in detail. The scatter plots in Figure 4 depict the relationships between BF impacts at different ERLs
261 for every source and model. IND is the source for which the similarity between the different ERLs is the highest with
262 regression slopes and R² between impacts calculated for the three ERLs of CAMx and the two of FARM near unity.
263 Although also the regressions between TRA impacts are linear, the 50% ERL impacts are ca. 8% lower and the 20%
264 ERL ca. 12% lower than those obtained with 100% ERL using the same model. The impacts at 50% and 20% ERLs
265 are well correlated, and the latter are less than 5% below the former for both CAMx and FARM values. For AGR the
266 relationship between the impacts calculated for both 50% and 20% ERLs are clearly non-linear when compared to
267 100% ERL. In the latter impacts are 3 or 4 times higher than the former two, especially for mid to high impacts. By
268 comparison, the relationship between impacts at 50% and 20% ERLs is closer to linearity (R² = 0.99), with the latter
269 leading to 18% - 20% lower impacts than the former. The results shown in Figure 4 confirm that AGR is the source
270 presenting the most serious non-linearity among those emitting SIA precursors (see Section 3.1). In addition, the
271 analysis indicates that also for TRA the impacts of the different ERLs are not fully equivalent.

272 The large differences in AGR impacts on PM₁₀ between 100% and the other ERLs are likely explained by two reasons.
273 Firstly, turning off AGR 100% systematically shifts the system into a different chemical regime, while this is not the
274 case for the other sources, and secondly, the influence of limiting precursors (leading to less than double counting and
275 consequently less BF overestimation with respect to TS) is not expressed at 100% ERL (Appendix A Section A2.2).
276 The differences between 50% and 20% ERLs could be explained by the way in which limited chemical regimes
277 interact with the reduction of emissions. Since the non-linearity associated with limited chemical regimes appears only
278 when the emission reduction causes a drop of concentrations higher than the excess of the non-limiting precursor
279 (Appendix A), the chance of such non-linearity to influence source impacts is proportional to the emission reduction.
280 However, the relatively small differences observed between 50% and 20% ERLs are likely due to the smoothing effect
281 of the NH₄NO₃ equilibrium with respect to the non-linearity caused by a limited chemical regime because such
282 equilibrium leads PM₁₀ concentrations to change even when the non-limiting precursor emission reduction is lower
283 than the excess (Appendix A Figure A1).

284 3.3 Interaction terms

285 In Figure 5 the annual average interaction terms (\hat{c}) of the factor decomposition, which are used in this study as
286 indicators of the impact's non-linearity, are mapped. The binary interaction terms are, in general, of higher magnitude
287 than the ternary interaction terms. The most negative interaction terms (indicating BF > TS) are observed in the 100%
288 ERL for the contemporary reduction of AGR and TRA in the rural areas located to the north of the Po Valley where
289 NH₃ is in excess, while the interaction terms are less negative in the main urban areas where NH₃ is a limiting factor.
290 When AGR and IND are both reduced 100%, the most negative interaction terms are observed in the industrial districts
291 around the main cities to the south of the Po Valley and to a lesser extent in the rural areas in the central Po Valley.
292 On the contrary, positive interaction terms are observed for the IND – TRA binary reduction due to the competition
293 between HNO₃ and H₂SO₄ that leads to an increase in the PM formation when SO₂ emissions (mainly industrial) are
294 reduced in presence of NO_x (deriving mainly from road transport). Such maximum positive interactions are observed
295 in vast areas of the central Po Valley. A similar geographical pattern of the interaction terms is observed for 50% and
296 20% ERL (Figures S8 and S9, respectively) with the magnitude of the interaction decreasing with the emission
297 reduction.



298

299 **Figure 5: Map of the binary and ternary interaction terms of the PM₁₀ factor decomposition for AGR, IND and TRA in the**
 300 **CAMx BF 100% scenarios.**

301 A similar analysis was carried with FARM at 50% ERLs for **residential heating** (Figure S10) and the resulting
 302 interaction terms were very low compared with those the other sources at the same ERL. The explanation is that
 303 despite the considerable contribution of this source to PM₁₀ its origin is mainly primary with a high non-reactive
 304 carbonaceous fraction (Piazzalunga et al., 2011) and therefore the impact on the secondary inorganic aerosol is limited.

305 The values of the interaction terms depend on the pollutant concentration. In order to define when \hat{c} is significantly
 306 different from zero, and consequently when the non-linearity is not negligible, the absolute value $|0.5|$ % BC is
 307 proposed. Such arbitrary threshold was defined to highlight the interactions that according to the analysis of the
 308 impacts presented in the previous sections are associated with evident non-linear situations (e.g. AGR-TRA). In
 309 Figures S11 and S12 are reported the maps of the interaction terms expressed as % of the base case for 100% and 50%
 310 ERLs, respectively. According to the proposed threshold, at 100% ERL most of the Po Valley fall in the area where
 311 non-linearity is measurable for all the binary and ternary interactions. At 50% ERL, the non-linearity of the binary
 312 interactions AGR-IND are measurable in industrial districts located to the SW and NW of the Po Valley including the
 313 industrial areas to the NW of Milan. The non-linearity associated to the interaction AGR-TRA is not negligible in the
 314 entire Po Valley and also in the Alpine areas, probably due to the low PM₁₀ levels of the latter. The binary interaction
 315 IND-TRA exceeds the threshold only in the central area of the Po valley and in a hot spot to the NW of Milan. The
 316 ternary interaction is below the threshold for the entire domain. For the 20% ERL (not shown) all the interactions are
 317 negligible according to CAMx while FARM provides a pattern comparable to the 50% ERL.

318 3.4 Analysis of chemical regimes

319 A more in-depth analysis of the relationships between the chemical regime and the interaction terms was accomplished
 320 in three selected sites with different source emission set up (their position is shown in Figure S1). A rural location at
 321 the border between the provinces of Cremona and Brescia (CR_P) was selected because of the high NH₃ emissions
 322 while the local NO_x and SO₂ emissions are very limited. The site of Milan (MI) was selected because representative
 323 of a typical urban situation with high NO_x concentrations deriving from road transport emissions. The NH₃ emissions
 324 in this site are very limited and are associated with road transport while also SO₂ emissions are low and derive in part

325 from the energy production. The third site is an industrial area in the province of Ravenna (RA_P) located in the
326 South-Eastern Po Valley. In this location, there are considerable SO₂ emissions from industry, which also release NO_x,
327 and moderate NH₃ emissions from the agricultural sector. In order to define the chemical regime in each base case
328 (CAMx and FARM) and each of the simulations including binary or ternary interactions, the gas ratio (GR) proposed
329 by Ansari and Pandis (1998) was used:

$$330 \quad GR = ([NH_3] + [NH_4^+] - 2[SO_4^{2-}]) / ([HNO_3] + [NO_3^-]) \quad (3)$$

331 where concentrations are nmol.m⁻³ or in nmol.mol of air (ppb).

332 The GR value defines three different chemical regimes:

- 333 (a) GR>1, in which NH₄NO₃ formation is limited by the availability of HNO₃,
- 334 (b) 0<GR<1, in which NH₄NO₃ formation is limited by the availability of NH₃, and
- 335 (c) GR<0, in which NH₄NO₃ formation is inhibited by H₂SO₄

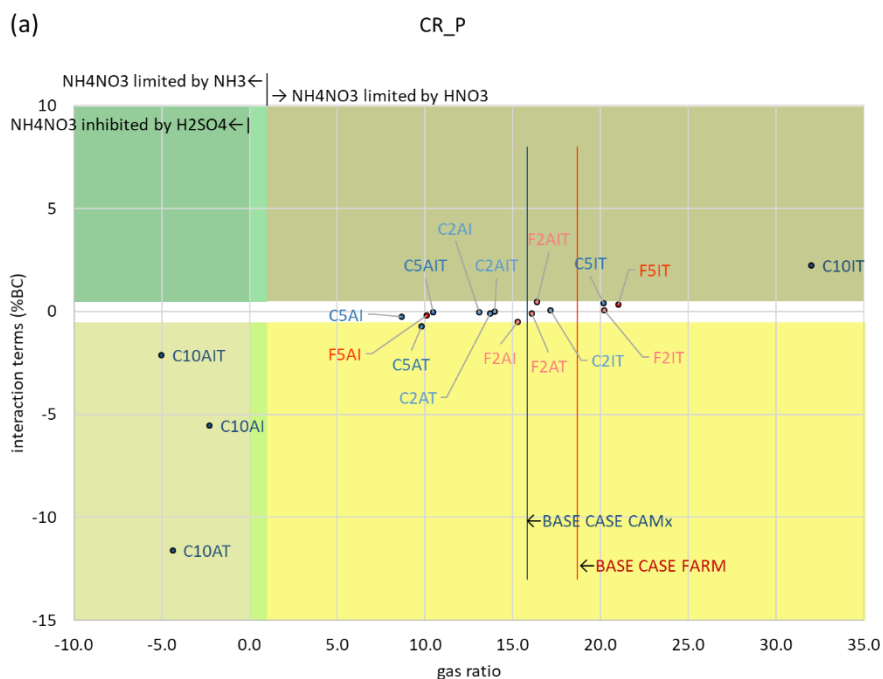
336 The plots in Figure 6 display for each scenario the magnitude of the changes in the chemical regime with respect to
337 the base case, and the relationship between such changes and the interaction terms (expressed as a percentage of the
338 PM yearly mean concentrations). Each plot is divided in zones defined by the combination of the gas ratio (GR)
339 thresholds, and the threshold proposed in this study for the interaction terms ($\hat{c} > |0.5\% \text{ BC}|$) as indicator of non-
340 negligible non-linearity in the mass concentration allocated to sources with respect to the PM mass concentration.

341 A common feature of all three sites is that the higher the ERL the higher the difference between the GR of the scenarios
342 and the one of the base case providing evidence about the extent to which the emission reductions alter the original
343 conditions. The points representing simulations in which AGR is reduced sit to the left of their respective base case.
344 The scenarios with 100% ERL often lead to changes in the chemical regime and to the highest absolute interaction
345 terms. On the other hand, 50% and 20% ERLs lead, in general, to \hat{c} values closer to zero than 100% ERL, indicating
346 lower or negligible non-linearity (located in the white background area). All interactions IND-TRA give rise to \hat{c}
347 values ≥ 0 , consistent with the competition effect (Appendix A Section A2.3). In CR_P and RA_P such simulations
348 lead to increase in GR (data points in Figure 6a and c are placed to the right of their base case), while in MI they lead
349 to null or slightly negative changes in GR (data points are located to the left of the base case in Figure 6b). This
350 behaviour indicates that the simultaneous reduction of IND and TRA leads to a higher impact of ammonia + nitric
351 acid on GR compared to the one of sulfate, in the three sites.

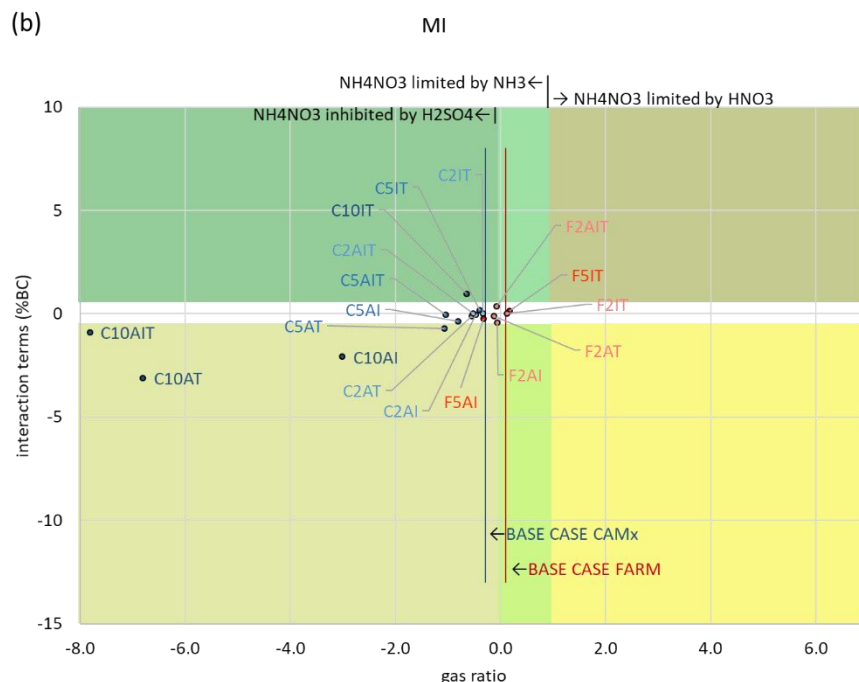
352 In CR_P the base cases of CAMx and FARM represent a HNO₃ limited chemical regime for NH₄NO₃ formation, in
353 line with the rural character of this area (Figure 6a). All scenarios where AGR is reduced lead to a decrease in GR
354 (points located to the left of the corresponding base case) indicating a loosening of the HNO₃ limitation, while all
355 those in which AGR is not reduced lead to an increase in GR (points located to the right of the corresponding base
356 case), indicating a stronger HNO₃ limitation. Sizeable negative \hat{c} are observed in scenarios reducing AGR 100%, likely
357 associated to the shift towards a NH₃ limited regime when AGR, the only significant source of this precursor, is turned
358 off. The described situation is reflected by the points representing the interaction terms AGR-IND (C10AI), AGR-
359 TRA (C10AT) and AGR-IND-TRA (C10AIT) of the 100% ERL located at the left-bottom of Figure 6a. The only
360 100% ERL scenario that does not lead to a chemical regime change is the contemporary reduction of IND and TRA
361 (C10IT). It also leads to positive interaction terms resulting from the competition between HNO₃ and H₂SO₄. In this
362 case, the abatement of SO₂ emissions leads to a reduced availability of H₂SO₄, which is replaced in the reaction with
363 NH₃ by HNO₃, the latter deriving from NO_x emissions also from other sectors on top of TRA and IND (e.g. energy
364 industry) which is an example of compensation process (Appendix A Section A2.5). Figure 6a shows that for 50%
365 and 20% ERLs, the emission reductions do not modify the chemical regime at this site. The AGR-TRA (C5AT) is the
366 only scenario at 50% ERL leading to a non-negligible \hat{c} value. The scenarios at the 20% ERL generally show similar
367 behaviours as those at 50%.

368 In MI the base case simulations correspond to a chemical regime where NH₄NO₃ is limited by NH₃ (Figure 6b). The
369 inhibition of NH₄NO₃ formation by H₂SO₄ is unclear since the GR values calculated from both models are close to
370 the boundary between H₂SO₄ inhibited and non-inhibited chemical regimes. As in the previous site, all scenarios with
371 100% ERLs (C10) but one (C10IT) lead to a situation with strong NH₃ limitation, H₂SO₄ inhibition and negative

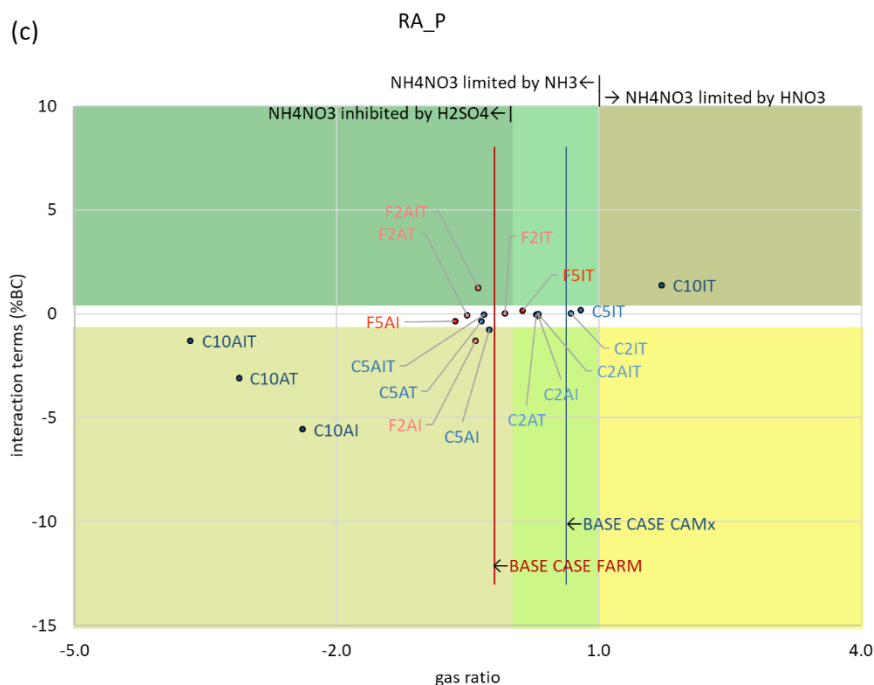
372 interaction terms (data points at the bottom left of Figure 6b). However, unlike the previous site, the combined 100%
 373 reduction of IND and TRA (C10IT) in MI leads to a H₂SO₄ limited regime. Thus, all 100% ERL scenarios lead to a
 374 strengthening of the H₂SO₄ inhibited chemical regime, which is relatively weak in the base case. As already observed
 375 in CR_P, the interaction terms at 50% and 20% ERLs are negligible, with the exception of AGR – TRA (C5AT).
 376 Among these scenarios, all those involving AGR reductions lead to regimes where NH₄NO₃ formation is limited by
 377 NH₃ and inhibited by H₂SO₄ (data points to the left of the corresponding base case). On the contrary, most scenarios
 378 not involving AGR (F5IT, F2IT, except C5IT) lead to situations where NH₄NO₃ formation is more limited by NH₃
 379 (data points to the right of the corresponding base case) while the inhibition by H₂SO₄ is uncertain since data points
 380 remain close to the boundary between the two regimes.



381



382



383

384 **Figure 6: Plot of the interaction terms ($\hat{\epsilon}$), expressed as percentage of the base case (BC), in three selected sites with different**
 385 **chemical regimes versus the gas ratio (Ansari and Pandis, 1998). a) CR_P: Cremona province, b) MI: Milan and c) RA_P:**
 386 **Ravenna province. C: CAMx and F: FARM. 10, 5 and 2 indicate the 100%, 50% and 20% ERLs, respectively. A:**
 387 **agriculture, I: industry and T: transport. White background indicates negligible interaction terms.**

388 In RA_P, both base cases are in a regime of NH_4NO_3 formation limited by NH_3 . However, for CAMx base case
 389 simulation NH_4NO_3 formation is not inhibited by H_2SO_4 while this is case for the FARM base case (Figure 6c). As in
 390 CR_P, the CAMx 100% scenarios in which AGR is reduced lead to decrease in GR and negative interaction terms

391 (data points at the bottom left), while the one involving the interaction IND-TRA (C10IT) leads to an increase in GR
392 and positive interaction term (data points at the top right). All scenarios in which AGR is reduced lead to NH₃
393 limitation and in most cases also H₂SO₄ inhibition chemical regimes (data points to the left of the respective base
394 case). On the contrary, the scenarios in which only combustion sources (TRA and IND) are reduced lead to regimes
395 where NH₄NO₃ formation is limited by NH₃ (data points to the right of the corresponding base case) and not inhibited
396 by H₂SO₄ (with some data points close to the boundary between the two regimes).

397 Among the scenarios at 50% and 20% ERLs, those involving AGR and IND lead to the highest absolute interaction
398 terms, of which some (C5AI, F2AI) are negative and clearly different from zero (non-linearity) with the exception of
399 F5AI that presents a negligible interaction term. The higher interaction terms for the AGR-IND scenarios with respect
400 to the other sites may be related to the greater importance of IND compared to TRA in this particular region.

401 The numerical relationship between the interaction terms and the gas ratio delta (i.e. the difference between the gas
402 ratio in one run and the corresponding base case) varies from site to site and, therefore, it is not possible to define
403 acceptability thresholds valid for the entire domain.

404 4. Conclusions

405 The theoretical analysis carried out by Clappier et al. (2017) applying factor decomposition was further developed in
406 this study by undertaking a real source apportionment exercise using CTM models in an area with a complex
407 meteorology and chemistry, namely the Po Valley.

408 The **interaction terms** of the factor decomposition measure the consistency between the impacts obtained with single
409 source reductions compared to those of multiple source reductions. Consequently, they are also suitable indicators of
410 the non-linearity between the sum of the sources' mass concentration and the PM₁₀ total mass concentration. In
411 addition, the **interaction terms used in association with the GR** provide evidence about the relationships between
412 changes in the chemical regime (e.g. limiting precursor, competition) and the non-linear response of PM₁₀
413 concentrations to emissions reductions.

414 The analysis of the single secondary inorganic constituents of PM₁₀ combined with interaction terms and GR made it
415 possible to identify a series of mechanisms that influence the non-linear response of these pollutants when emission
416 reduction scenarios are applied to a real particulate pollution case: near double counting, precursor- limited chemical
417 regime, competition between precursors, thermodynamic equilibrium and compensation.

418 The results of this study confirm that due to the key role of NH₃ in the formation of SIA in the Po Valley, the **strongest**
419 **non-linear response of PM₁₀ concentrations to emissions reductions is associated with the AGR-TRA reduction**
420 **scenarios**. The differences in PM₁₀ attributed to AGR applying the TS and the BF approaches at 100% emission
421 reduction level **reach a factor 2**. Moreover, the competition between HNO₃ and H₂SO₄ to react with NH₃ leads to a
422 modest non-linear response of PM₁₀ in scenarios where TRA and IND are reduced simultaneously, especially in areas
423 with important SO₂ emissions. Tests carried out in the study area about RES indicate a very little non-linearity
424 associated with this source, likely due to the dominance of the primary fraction, including a considerable amount of
425 carbonaceous constituents.

426 The factors that trigger differences in SA between the TS and the BF approaches also lead to **non-linearity among**
427 **different levels of emission reduction**. For PM₁₀, this non-linearity is higher between 100% and the other reduction
428 levels and is mainly observed in scenarios involving AGR reductions where the differences may reach a factor of 3-
429 4, and to a lesser extent to scenarios involving TRA where differences are ca. 10%. This is due to a) the almost
430 complete suppression of NH₃ when turning off AGR while turning off TRA leaves other strong sources of SO₂ and
431 NO_x active, and b) the fact that limiting precursors' effect is only observable for ERL below 100%. Moreover, the
432 present study shows that even when the **secondary inorganic components of PM₁₀ present a non-linear behaviour**
433 in their annual averages, the PM₁₀ response may result linear due to the compensation between different constituents.

434 It was also observed that in the majority of the tested scenarios at 50% and 20% ERLs, interaction terms are either
435 negligible or remain low (a few percent of the base case concentrations). In these conditions, the TS and the BF
436 approaches provide comparable results. Such findings were confirmed in this study by the direct comparison between
437 these two approaches that provided highly comparable spatial patterns and quantification of the role (contribution or
438 impact) of IND, TRA and RES sources.

439 Due to its high emission levels and stagnation of air masses, the situations potentially leading to non-linear responses
440 are common in the Po Valley making this region particularly suitable to study this kind of phenomena. The results of
441 the study suggest that AGR is the most important source from this point of view: a number of scenarios involving the
442 reduction of emission from AGR lead to non-linear responses of PM_{10} . This is due to the key role of NH_3 , whose only
443 significant source is AGR, in the formation of secondary inorganic aerosol (SIA) in the test area. In addition, scenarios
444 with high AGR emissions reduction (e.g. 100%) lead to a shift of the NH_4NO_3 formation chemical regime. One of the
445 implications of these findings is that when there is a strong non-linear response (e.g. 100% reduction of AGR) it is
446 not appropriate to sum the impacts obtained with single source reductions to estimate the combined effect of more
447 than one source, Furthermore, in case of AGR emission reduction extrapolating the results of moderate ERL scenarios
448 to stronger ERL (e.g. greater than 50%, as shown in Figure 4) is discouraged too. Likewise, in such situations, the use
449 of TS results to derive information about emission reduction impact can be misleading.

450 The findings of the present work about PM_{10} are also valid for the behaviour of $PM_{2.5}$. In the runs used for this study
451 these two size fractions present the same geographical patterns and values because the difference between them (the
452 coarse fraction) is mainly primary and thus expected to respond linearly to emissions reduction.

453 Considering the complexity of computing the Stein and Alpert decomposition for all the possible combinations of
454 source reductions (due to the high number of required runs), this work aims to provide a picture of the conditions that
455 give rise to non-linear response of PM_{10} or $PM_{2.5}$ yearly averages for the reduction of single sources. Such picture is
456 intended as a contribution to simplify the tests needed in common modelling practice to detect non-linear responses
457 by allowing practitioners to focus on the situations that are more likely to be associated with non-linearity.

458 BF and TS are different but complementary techniques. Understanding how they work is necessary to adopt the one
459 which is most suitable for the purposes of the work. On the one hand, BF is the best choice to assess the response of
460 the air quality system to changes in the emission rates. For instance, this approach emphasises better the key role of
461 agriculture and is then most suitable for planning purposes. On the other hand, TS is most valuable when the focus is
462 on the actual mass transferred from sources to receptors in the situation described in the base case. It is, therefore,
463 most appropriate for studying the health impact of sources because the effect of pollutants depends on the dose. An
464 option to emphasise the role of agriculture with this approach would be to develop a version based on the molar ratios
465 instead of the mass. However, assessing the usefulness of such approach would require a new full set of tests.

466 One of the main outcomes of this study is that in most situations (linear response) the two approaches provide similar
467 results for the annual averages, which is the time averaging required for long-term air quality indicators. However, for
468 shorter time windows (daily, seasonal averages or pollution episodes) non-linearity is likely be more prominent. If
469 there is a clear non-linear response, precaution is needed in the interpretation of the results from both approaches:

- 470 - in BF it is not appropriate to sum of the impact of the sources obtained by single source reduction because
- 471 they may not match the total PM, while
- 472 - in TS there could be a distortion in the allocation of secondary aerosol because it does not account for indirect
- 473 effects (Mircea et al, 2020; Thunis et al., 2019).

474 Moreover, in case of non-linear responses, also extending the results of BF for a specific ERL to another (e.g. 20 to
475 50 or 100%) could be misleading.

476 To overcome the limitations of strong non-linear responses on source apportionment the only option is to run a
477 scenario analysis with the exact combination of emission reductions for all the sources at once so all the interactions
478 among them leading to secondary compounds are accounted for. However, this approach is valid only for one specific
479 situation.

480 The methodology proposed in this study provides the means to identify non-linear responses to promote a more
481 mindful use of source apportionment techniques. The ultimate goal of which is to inform more effective air quality
482 plans with a consequent more efficient use of economic resources and a faster achievement of air quality standards to
483 protect human health and ecosystems.

484 **5. Code and data availability**

485 The model code and data used for the calculations and figures presented in this paper are available at
486 <http://doi.org/10.5281/zenodo.4306182>.

487 **6. Author contribution**

488 C.A. Belis: conceptualisation, formal analysis, methodology, visualisation, writing – original draft preparation; G.
489 Pirovano: conceptualisation, formal analysis, review & editing; M.G. Villani: formal analysis, visualization, review
490 & editing; G. Calori: formal analysis, visualization, review & editing; N. Pepe: formal analysis, visualization, review
491 & editing; J.P. Putaud: conceptualisation, methodology, validation, review and editing

492 **7. Competing interests**

493 The authors declare that they have no conflict of interest

494 **8. Acknowledgements**

495 The authors acknowledge Kees Cuvelier for the development of a tool for the data elaboration and to Alain Clappier
496 and Philippe Thunis for the discussions during the preparatory phase of this work.

497 **9. References**

498 Ansari, A. S. and Pandis, S. N.: Response of Inorganic PM to Precursor Concentrations, *Environ. Sci. Technol.*, 32,
499 2706–2714, 1998.

500 ARIA Technologies and ARIANET: Emission Manager - Processing system for model-ready emission input - User's
501 guide. ARIA/ARIANET R2013.19, Milano, Italy, 2013.

502 ARIANET: FARM (Flexible Air quality Regional Model) - Model formulation and user manual -Version 4.13.
503 ARIANET R2018.22, Milano, Italy' 2019.

504 Belis, C.A., Cancelinha, J., Duane, M., Forcina, V., Pedroni, V., Passarella, R., Tanet, G., Douglas, K., Piazzalunga,
505 A., Bolzacchini, E., Sangiorgi, G., Perrone, M.G., Ferrero, L., Fermo, P., Larsen, B.R.: Sources for PM air
506 pollution in the Po Plain, Italy: I. Critical comparison of methods for estimating biomass burning
507 contributions to benzo(a)pyrene. *Atmospheric Environment* 45, 7266-7275, 2011.

508 Belis C. A., D. Pernigotti, G. Pirovano ,O. Favez, J.L. Jaffrezo, J. Kuenen, H. Denier van Der Gon, M. Reizer, V.
509 Riffault, L. Y. Alleman, M. Almeida, F. Amato, A. Angyal, G. Argyropoulos, S. Bande, I. Beslic, J-L.
510 Besombes, M.C. Bove, P. Brotto, G. Calori, D. Cesari, C. Colombi, D. Contini, G. De Gennaro, A. Di Gilio,
511 E. Diapouli, I. El Haddad, H. Elbern, K. Eleftheriadis, J. Ferreira, M. Garcia Vivanco,, S. Gilardoni, B. Golly,
512 S. Hellebust, P.K. Hopke, Y. Izadmanesh , H. Jorquera, K. Krajsek, R. Kranenburg, P. Lazzeri, F. Lenartz,
513 F. Lucarelli, K. Maciejewska, A. Manders, M. Manousakas, M. Masiol, M. Mircea, D. Mooibroek, S. Nava,
514 D. Oliveira,, M. Paglione, M. Pandolfi, M. Perrone, E. Petralia, A. Pietrodangelo, S. Pillon, P. Pokorna, P.

515 Prati, D. Salameh, C. Samara, L. Samek, D. Saraga, S. Sauvage, M. Schaap, F. Scotto, K. Sega, G. Siour, R.
516 Tauler, G. Valli, R. Vecchi, E. Venturini, M. Vestenius, A. Waked., E. Yubero : Evaluation of receptor and
517 chemical transport models for PM₁₀ source apportionment. *Atmospheric Environment X*, 5 100053, 2020.

518 Binkowski, F.S. and Roselle, S.J.: Models-3 Community Multiscale Air Quality (CMAQ) model aerosol component
519 1. Model description. *J. Geophys. Res.* 108: 4183, doi: 10.1029/2001JD001409, 2003.

520 Carter, W.P.L.: Documentation of the SAPRC-99 Chemical Mechanism for VOC Reactivity Assessment. Final Report
521 to California Air Resources Board, Contract 92-329 and 95-308, SAPRC, University of California, Riverside,
522 CA, 2000.

523 Clappier, A., Belis, C.A., Pernigotti, D., Thunis, P.: Source apportionment and sensitivity analysis: Two
524 methodologies with two different purposes. *Geoscientific Model Development* 10, 4245-4256, 2017.

525 EEA, Air quality in Europe – 2019 report. EE Report 10/2019, doi:10.2800/822355, 2019

526 ENVIRON: CAMx (Comprehensive Air Quality Model with extensions) User’s Guide Version 5.4. ENVIRON
527 International Corporation, Novato, CA, 2011.

528 ENVIRON: CAMx (Comprehensive Air Quality Model with extensions) User’s Guide Version 6.3. ENVIRON
529 International Corporation, Novato, CA, 2016.

530 INEMAR - Arpa Lombardia: INEMAR, Emission Inventory: 2012 emission in Region Lombardy - public review.
531 ARPA Lombardia Settore Aria, <http://www.inemar.eu/>, 2015.

532 INERIS: Documentation of the chemistry-transport model CHIMERE [version V200606A]. Available at:
533 <http://euler.lmd.polytechnique.fr/chimere/>, 2006.

534 Karamchandani, P., Long, Y., Pirovano, G., Balzarini, A., Yarwood, G.: Source sector contributions to European
535 ozone and fine PM in 2010 using AQMEII modeling data. *Atmos. Chem. Phys.* 17, 5643–5664, 2017.

536 Kieseewetter G., Borken-Kleefeld J., Schöpp W., Heyes C., Thunis P., Bessagnet B., Terrenoire E., Fagerli H., Nyiri
537 A., and Amann M.: Modelling street level PM10 concentrations across Europe: source apportionment and
538 possible futures, *Atmos. Chem. Phys.*, 15, 1539-1553, 2015.

539 Lange, R.: Transferability of a three-dimensional air quality model between two different sites in complex terrain, *J.*
540 *Appl. Meteorol.*, 78, 665–679, 1989.

541 Larsen, B.R., Gilardoni, S., Stenström, K., Niedzialek, J., Jimenez, J., Belis, C.A.: Sources for PM air pollution in the
542 Po Plain, Italy: II. Probabilistic uncertainty characterization and sensitivity analysis of secondary and primary
543 sources. *Atmospheric Environment* 50, 203-213, 2012.

544 Manders, A. M. M., Bultjes, P. J. H., Curier, L., Denier van der Gon, H. A. C., Hendriks, C., Jonkers, S., Kranenburg,
545 R., Kuenen, J. J. P., Segers, A. J., Timmermans, R. M. A., Visschedijk, A. J. H., Wichink Kruit, R. J., van
546 Pul, W. A. J., Sauter, F. J., van der Swaluw, E., Swart, D. P. J., Douros, J., Eskes, H., van Meijgaard, E., van
547 Ulft, B., van Velthoven, P., Banzhaf, S., Mues, A. C., Stern, R., Fu, G., Lu, S., Heemink, A., van Velzen, N.,
548 and Schaap, M.: Curriculum vitae of the LOTOS–EUROS (v2.0) chemistry transport model, *Geosci. Model*
549 *Dev.*, 10, 4145-4173, 10.5194/gmd-10-4145-2017, 2017.

550 Mircea M., Calori G., Pirovano G., Belis C.A.: European guide on air pollution source apportionment for particulate
551 matter with source oriented models and their combined use with receptor models, EUR 30082 EN,
552 Publications Office of the European Union, Luxembourg, ISBN 978-92-76-10698-2, doi:10.2760/470628,
553 JRC119067, 2020.

554 Nenes, A, Pilinis, C., Pandis, S.N.: ISORROPIA: A New Thermodynamic Model for Multiphase Multicomponent
555 Inorganic Aerosols. *Aquatic Geochemistry*, 4, 123-152, 1998.

556 O'Brien, J.J.: A note on the vertical structure of the eddy exchange coefficient in the planetary boundary layer. *Journal of the atmospheric science* 27, 1213-1215, 1970.
557

558 Pepe N., G. Pirovano, A. Balzarini, A. Toppetti, G.M. Riva, F. Amato, G. Lonati: Enhanced CAMx source
559 apportionment analysis at an urban receptor in Milan based on source categories and emission regions,
560 *Atmospheric Environment: X*, Volume 2. <https://doi.org/10.1016/j.aeaoa.2019.100020>, 2019.

561 Pernigotti, D., Thunis, P., Cuvelier, C., Georgieva, E., Gsell, A., De Meij, A., Pirovano, G., Balzarini, A., Riva, G.M.,
562 Carnevale, C., Pisoni, E., Volta, M., Bessagnet, B., Kerschbaumer, A., Viaene, P., De Ridder, K., Nyiri, A.,
563 Wind, P.: POMI: a model inter-comparison exercise over the Po Valley. *Air Qual Atmos Health*. DOI
564 10.1007/s11869-013-0211-1, 2013.

565 Piazzalunga, A., Belis, C., Bernardoni, V., Cazzuli, O., Fermo, P., Valli, G., Vecchi, R. Estimates of wood burning
566 contribution to PM by the macro-tracer method using tailored emission factors. *Atmospheric Environment*
567 45, 6642-6649, 2011.

568 Pültz, J., Banzhaf, S., Thürkow, M., Kranenburg, R., Schaap, M.: Source attribution of PM for Berlin using Lotos-
569 Euros. 19th International Conference on Harmonisation within Atmospheric Dispersion Modelling for
570 Regulatory Purposes, Harmo 2019, 2019.

571 Schell, B., Ackermann, I. J., Hass, H., Binkowski, F. S., and Ebel, A.: Modeling the formation of secondary organic
572 aerosol within a comprehensive air quality model system, *J. Geophys. Res.*, 106, 28275–28293, 2001.

573 Skamarock, W.C., Klemp, J.B., Dudhia, J., Gill, D.O., Barker, D.M., Duda, M.G., Huang, X.Y., Wang, W., Powers,
574 J.G.: A Description of the Advanced Research WRF Version 3. NCAR Technical Note NCAR/TN-475pSTR,
575 Boulder, Colorado, 2008.

576 Stein U. and Alpert P. Factor separation in numerical simulations, *Journal of the Atmospheric Sciences*, 50 (4), 2107-
577 2115, 1993.

578 Thunis P., Clappier A., Pisoni E., Degraeuwe B.: Quantification of non-linearities as a function of time averaging in
579 regional air quality modeling applications, *Atmospheric Environment*, 103, 263-275, 2015.

580 Thunis, P., Degraeuwe, B., Pisoni, E., Ferrari, F., and Clappier, A.: On the design and assessment of regional air
581 quality plans: The SHERPA approach, *J. Environ. Manag.*, 183, 952–958, 2016.

582 Thunis, P., Clappier, A., Tarrason, L., Cuvelier, C., Monteiro, A., Pisoni, E., Wesseling, J., Belis, C.A., Pirovano, G.,
583 Janssen, S., Guerreiro, C., Peduzzi, E.: Source apportionment to support air quality planning: Strengths and
584 weaknesses of existing approaches. *Environment International* 130, 104825, 2019.

585 UNC: SMOKE v3.5 User's manual. Available at: <http://www.smoke-model.org/index.cfm>, 2013.

586 Van Dingenen, R., Dentener, F., Crippa, M., Leitao, J., Marmer, E., Rao, S., Solazzo, E., Valentini, L.: TM5-FASST
587 a global atmospheric source–receptor model for rapid impact analysis of emission changes on air quality and
588 short-lived climate pollutants. *Atmos. Chem. Phys.* 18, 16173-16211, 2018.

589 WHO: Ambient air pollution: a global assessment of exposure and burden of disease. ISBN 9789241511353, 2016.

590 WHO: World health statistics 2018: monitoring health for the SDGs, sustainable development goals. Geneva: World
591 Health Organization. ISBN 978-92-4-156558-5. Licence: CC BY-NC-SA 3.0 IGO, 2018.

592 Yarwood G., Morris, R.E., Wilson, G.M.: Particulate Matter Source Apportionment Technology (PSAT) in the CAMx
593 Photochemical Grid Model. Proceedings of the 27th NATO/ CCMS International Technical Meeting on Air
594 Pollution Modeling and Application. Springer Verlag, 2004.

595 Yarwood, G., Rao, S., Yocke, M., Whitten, G.: Updates to the Carbon Bond Chemical mechanism: CB05, report, Rpt.
596 RT-0400675, US EPA, Res. Tri. Park, 2005.

597 Appendix A

598 A1) Interaction terms

599 The interaction terms in the factor decomposition (Stein and Alpert, 1993) reflect the consistency between single
600 source emission reduction and contemporary reduction of more than one source and are indicators of the non-linear
601 response of particulate matter (PM₁₀ or PM_{2.5}) concentration to single source reductions.

602 A1.1) Binary interactions

603 Binary interactions describe the situation of two precursors α and β emitted by two different sources A and B,
604 respectively, that react in atmosphere to form the secondary compound γ ($\alpha + \beta \rightarrow \gamma$). ΔC denotes the change in the
605 concentration of γ as a consequence of applying the same percentage of reduction to sources A and B separately or at
606 the same time. The binary interaction term (\hat{c}_{AB}) is the difference between $\Delta C(\gamma)$ due the contemporary reduction of
607 both sources and the sum of $\Delta C(\gamma)$ due to the reduction of each single source:

$$608 \hat{c}_{AB} = \Delta C_{AB} - \Delta C_A - \Delta C_B \quad (A1)$$

609 A1.2) Ternary interactions

610 By analogy, ternary interactions refer to the interplay of three sources A, B and C each emitting one precursor
611 (α , β and χ , respectively) which react among each other in atmosphere for example as follows:



615 The ternary interaction term is a function of $\Delta C(\gamma)$ resulting from the reduction of all three sources at once, of $\Delta C(\gamma)$
616 resulting from the reduction of each single source at a time, and of the \hat{c} for all the combinations of binary source
617 reductions as described below (see also eq. 1):

$$618 \hat{c}_{ABC} = \Delta C_{ABC} - \Delta C_A - \Delta C_B - \Delta C_C - \hat{c}_{AB} - \hat{c}_{AC} - \hat{c}_{BC} \quad (A5)$$

619 A2) Situations giving rise to non-linearity

620 This section analyses in detail the situations that may lead to non-linearity. Most of these situations are visible in
621 binary interactions, however, competition is only observable in ternary interactions. The different binary interactions
622 that are part of ternary interactions may represent different situations described in this section, some of which
623 leading to non-linearity and others not.

624 A2.1) Double counting

625 This interaction takes place when the concentrations of the emitted precursors (α , β) are close to the stoichiometric
626 ratios and consequently none of them is limiting the reaction or is in excess. In addition, no compensation mechanisms
627 (see Section A2.5) take place and there are no other precursors competing for the reaction between α and β . Under
628 these circumstances, the application of the brute force (BF) approach leads to a 100% reduction of the concentration
629 of γ when reducing the emissions of either source A or B by 100%. This is called “**double counting**” because the sum
630 of the scenario where only A is reduced by 100% and the one where only B is reduced by 100% is exactly the double
631 of the mass of the scenario when both sources A and B are reduced at once. This situation is described in the equation
632 below:

633 $\Delta C_{AB} = 1/2 (\Delta C_A + \Delta C_B)$ (A6)

634 in other words, the ΔC of the contemporary reduction of A and B is the half of the sum of the ΔC of the single
 635 reductions of A and B, respectively. In this situation, \hat{c}_{AB} is negative and its absolute value is the highest and is equal
 636 to the ΔC of A and B, which are equal to each other.

637 $\hat{c}_{AB} = -\Delta C_A = -\Delta C_B = -1/2 (\Delta C_A + \Delta C_B)$ (A7)

638 A perfect double counting is a theoretical situation that does not take place in the “real-world” formation of secondary
 639 inorganic aerosol (SIA) because of the influence of other factors such as reversible reactions and pH feedback on
 640 solubility (deliquescent particles). Consequently, in this study we observe situations **near to double counting** where
 641 the interaction terms are strongly negative, like the one described below.

642 Let’s consider the reaction $\text{NH}_3 + \text{HNO}_3 \rightarrow \text{NH}_4\text{NO}_3$, where A is the source of NH_3 and B is the one of HNO_3 and
 643 concentrations in ppb are denoted by $[\text{NH}_3] = a$ and $[\text{NO}_3] = b$. When setting Gas Ratio (GR, Ansari & Pandis, 1998)
 644 = 1, $[\text{SO}_4^{2-}] = 0.5$ ppb (about $2 \mu\text{g}\cdot\text{m}^{-3}$) and assume particles to be deliquescent, then $d[\text{PM}]/d[\text{NH}_3] = 2.5$ and
 645 $d[\text{PM}]/d[\text{NO}_3] = 0.6$. Under these circumstances, a 50% reduction of source A leads to a decrease in PM of $\Delta C_A = 2.5$
 646 $\times a/2$; a 50% reduction of source B leads to a decrease in PM of $\Delta C_B = 0.6 \times b/2$; and a simultaneous 50% decrease of
 647 emissions from both A and B leads to a PM decrease of $\Delta C_{AB} = a/2 + b/2$. The actual interaction term is:

648 $\hat{c}_{AB_actual} = \Delta C_{AB} - \Delta C_A - \Delta C_B = -0.75 a + 0.2 b$

649 while according to eq. (A7) the double counting interaction term is $\hat{c}_{AB_DC} = -0.625 a - 0.15 b$

650 Since near the stoichiometric ratio a is similar to b , the actual interaction term is close to but less negative than the
 651 double counting interaction term.

652 **A2.2) Precursor limited chemical regime**

653 Most commonly, the concentrations of the precursors significantly differ from the stoichiometric ratio and
 654 consequently one of them acts as limiting factor or limiting precursor (in the example below the one emitted by source
 655 A, which implies $\Delta C_A > \Delta C_B$). In this case, the emission reduction can lead to two different situations:

656 2.2a) the reduction of the emissions causes a decrease of the non-limiting precursor (β) concentration lower or
 657 equal to the its excess with respect to the limiting precursor (α) leading to an interaction equal to zero because
 658 ΔC_B is zero and $\Delta C_{AB} = \Delta C_A$.

659 $\hat{c}_{AB} = \Delta C_{AB} - \Delta C_A - \Delta C_B = 0$ (A8)

660 In this case **the potential interaction does not take place**

661 2.2b) the reduction of the emissions of source B is enough to reduce the concentration of precursor β by more
 662 than its excess with respect to α leading to a negative \hat{c}_{AB} with lower absolute value than the double counting.

663 $0 > \hat{c}_{AB} > -1/2(\Delta C_A + \Delta C_B)$ (A9)

664 In this case there is a situation of **less than double counting**

665 Less than double counting is an intermediate situation between no interaction and the maximum interaction which is
 666 the double counting and the interaction terms are always negative.

667 The limitation regime can only be observed when source reductions are less than 100% because, unless the same
 668 precursor is emitted by other sources or transported from other areas (see Section A2.5), the complete removal of the
 669 precursor leads to the complete removal of its products.

670 In the real world, situations where NH_4NO_3 formation is limited by free NH_3 availability ($\text{GR}<1$) or total nitrate
 671 availability ($\text{GR}>1$) are common. However, due to feedback processes, the impact of reducing the emissions of a non-
 672 limiting precursor is small but not null, while the one of reducing the emissions of a limiting precursor may be
 673 smoothed by the NH_4NO_3 equilibrium (see Section A2.4).

674 **A2.3) Competition**

675 The interaction between two sources A and B can be affected by a third one C when the precursors emitted by the two
 676 sources B and C compete to react with the one emitted by source A (See eqs. A2 and A3). In the formation of SIA,
 677 there is competition between HNO_3 and H_2SO_4 to react with NH_3 to produce ammonium nitrate and ammonium
 678 sulfate, respectively. HNO_3 derives from NO_x emissions emitted i. a. by road transport (there are other sources),
 679 H_2SO_4 mainly comes from SO_2 emitted by industry, and NH_3 is mainly emitted from agriculture.

680 In situations where the formation of SIA is not limited neither by H_2SO_4 nor by HNO_3 availability (and conditions are
 681 favourable to the formation of $(\text{NH}_4)_2\text{SO}_4$), the reaction $\text{H}_2\text{SO}_4 + \text{NH}_3$ produces 1 mol of $(\text{NH}_4)_2\text{SO}_4$ every 2 mols of
 682 NH_3 while the reaction $\text{HNO}_3 + \text{NH}_3$ produces 1 mol of NH_4NO_3 for every mol of NH_3 . The yield of aerosol in terms
 683 of mols of the second reaction is twice the one of the first reaction. The difference of mass in $\mu\text{g}/\text{m}^3$ is as follows:

684 The reaction $2 \text{NH}_3 + \text{H}_2\text{SO}_4 \rightarrow (\text{NH}_4)_2\text{SO}_4$ leads to $3.9 \mu\text{g}.\text{m}^{-3}$ PM from $1 \mu\text{g}.\text{m}^{-3}$ NH_3 .

685 The reaction $\text{NH}_3 + \text{HNO}_3 \rightarrow \text{NH}_4\text{NO}_3$ leads to $4.7 \mu\text{g}.\text{m}^{-3}$ PM from $1 \mu\text{g}.\text{m}^{-3}$ NH_3 .

686 Consequently, when the SO_2 emissions are reduced in an NH_3 -limited regime and HNO_3 replaces H_2SO_4 to react with
 687 NH_3 there is an increase in the PM concentration.

688 In order to quantify the abovementioned competition it is necessary to compute the interaction between at least three
 689 sources at once (eq. A5).

690 The competition in a three-source system may lead to negative ΔC (= increase in PM_{10}) for the single IND reduction
 691 scenarios which results in positive binary IND-TRA interaction terms (see Section 3.4). The effect is also observed in
 692 the TRA impact on sulfate and the IND impact on nitrate.

693 **A2.4) Equilibrium with solid NH_4NO_3**

694 The analysis of the previous cases is valid for unidirectional or irreversible chemical reactions. However, in the
 695 atmosphere the reaction products, nitrate and ammonium, are in thermodynamic equilibrium with the reagents
 696 ammonia and nitric acid:



698 The actual concentrations of reagents and products depends on the ratio between the kinetics of the reaction in either
 699 direction. For the conditions in which particulate ammonium nitrate is in solid state (non-deliquescent particles), the
 700 equilibrium constant K of this reaction is the product of the reagent gas phase concentrations $[\text{HNO}_3(\text{g})]$ and $[\text{NH}_3(\text{g})]$:

$$701 K = [\text{HNO}_3(\text{g})] [\text{NH}_3(\text{g})] \quad (\text{A11})$$

702 Any emission reduction leading to decreases in HNO_3 and/or NH_3 gas phase concentrations by a factor q shall lead to
 703 the shifting of the equilibrium towards the gas phase (volatilisation) of a concentration of ammonium nitrate ΔC so
 704 that the equilibrium ($K = [\text{HNO}_3(\text{g})] \times [\text{NH}_3(\text{g})]$) is reached again.

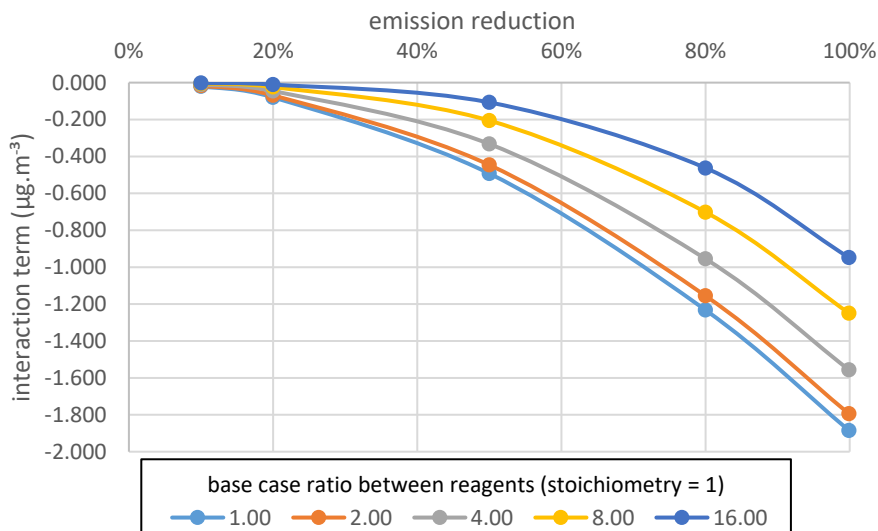
705 If in the base case, the concentrations of the reagents are $a = [\text{NH}_3(\text{g})]$ and $b = [\text{HNO}_3(\text{g})]$:

$$706 \text{In case only the source of ammonia (A) is reduced, } \Delta\text{C} = \Delta\text{C}_A \text{ with } K = (b + \Delta\text{C}_A) (a/q + \Delta\text{C}_A) \quad (\text{A12})$$

$$707 \text{In case only the source of nitric acid precursors (B) is reduced, } \Delta\text{C} = \Delta\text{C}_B \text{ with } K = (b/q + \Delta\text{C}_B) (a + \Delta\text{C}_B) \quad (\text{A13})$$

$$708 \text{In case both sources are reduced, } \Delta\text{C} = \Delta\text{C}_{AB} \text{ with } K = (a/q + \Delta\text{C}_{AB}) (b/q + \Delta\text{C}_{AB}) \quad (\text{A14})$$

709 Solving these second order equations for different emission reductions (represented by q in eq. A 12-14) shows that
 710 the inequality $\Delta C_{AB} < \Delta C_A + \Delta C_B$ (i.e. $\hat{c}_{AB} < 0$) is always observed (Figure A1). Moreover, the interaction terms vary
 711 in a non-linear way with respect to the emission reduction becoming less negative when the system moves away from
 712 stoichiometric conditions (Figure A1).



713
 714 **Figure A1: Variation of the interaction terms as a function of the NH₃ and HNO₃ emissions reduction for different**
 715 **stoichiometric ratios ranging from non-limited regime (r=1) to strongly limited regime (r=16). Calculations were performed**
 716 **for conditions in which K = 4 ppb².**

717 A2.5) Compensation

718 In addition to the determinants described in the previous sections, which are mainly associated with the modellistic
 719 approaches used to estimate source impacts and with atmospheric chemistry, there are other factors that may alter the
 720 linearity of the relationship between the emission reductions ΔE and the response ΔC . In this section, we generically
 721 refer to such alterations as compensation.

722 Compensation are all the processes taking place in real world conditions which alter the ΔC expected to result from a
 723 given ΔE in a theoretical exercise (either at the single cell or at the entire grid level), leading to interaction terms
 724 different from those expected only on the basis of applied emission reduction.

725 **Compensation of precursor emissions:** the actual emission reduction (ΔE) of one precursor is lower than the
 726 expected ΔE in a system with few sources because in a complex system, like the one analysed in this study, there are
 727 other sources of the same precursor in the grid. Consequently, the reduction of its concentration (ΔC) may not be
 728 proportional to the reduction (ΔE) of one emission source.

729 **Compensation of precursor concentrations:** the actual ΔC is different from the one expected from ΔE because there
 730 is import (advection) of this precursor from neighbouring grid cells or export (advection or deposition) from the
 731 considered grid cell.

732 Below are presented examples on how the compensation may affect the interaction terms in different chemical
 733 regimes.

734 a) The compensation alters the excess of the non-limiting precursor when emissions from not-considered sources or
 735 advection from other cells contribute significantly to the concentration of this precursor and consequently prevent the
 736 applied emission reduction from triggering a non-linear response (see Section A2.2).

737 b) The compensation alters the chemical regime. This can occur in different ways.

738 b1) Emissions from not-considered sources or advection processes are such that they keep the concentration of a
739 limiting precursor at the stoichiometric ratio with other precursors leading to larger negative interactions terms than
740 those expected (see Section A2.1).

741 b2) Advection or deposition processes may reduce the level of a non-limiting precursor to levels close to the
742 stoichiometric ratio with other precursors and consequently lead to more negative interaction terms as described in
743 Section A2.1.

744 b3) Compensation may also alter the concentration of a precursor which is in competition with another. For instance,
745 when the emissions from three major sources (e.g. AGR, TRA, IND) are reduced, other sources (e.g. energy industry,
746 residential heating) may become predominant in controlling the chemical regime of SIA formation, which may result
747 in novel inhibition or competition situations (e.g. Section A2.4).